BULLETIN OF THE POLISH ACADEMY OF SCIENCES
TECHNICAL SCIENCES, Vol. 68, No. 6, 2020
DOI: 10.24425/bpasts.2020.135379

Optimization on friction and wear behaviour of Al-Si alloy reinforced with B_4C particles by Powder Metallurgy using Taguchi design

R. JEYA RAJ[1], LENIN W.A. ANSELM[2], M. JINNAH SHEIK MOHAMED[2],
S. CHRISTOPHER EZHIL SINGH[3]*, T.D. JOHN[3], D. RAJEEV[4], G. GLAN DEVADHAS[5],
K.G. JAYA CHRISTYAN[6], R. MALKIYA RASALIN PRINCE[7], R.B. JEEN ROBERT[8]

[1] Department of Mechanical Engineering, Marthandam College of Engineering and Technology, Marthandam, Kanyakumari, Tamilnadu, India
[2] Engineering Department, Mechanical Section, University of Technology and Applied Sciences-Shinas, Sultanate of Oman
[3] Department of Mechanical Engineering, Vimal Jyothi Engineering College, Chemperi, Kannur, Kerala, India
[4] Department of Mechanical Engineering, Mar Ephram College of Engineering and Technology, Marthandam, Kanyakumari, Tamilnadu, India
[5] Department of Applied Electronics and Instrumentation Engineering, Vimal Jyothi Engineering College, Chemperi, Kannur, Kerala, India
[6] Department of Mechanical Engineering, Ramaiah Institute of Technology, Bangalore, Karnataka, India
[7] Department of Mechanical Engineering, Karunya Institute of Technology, Coimbatore, Tamil nadu, India
[8] Department of Mechanical Engineering, AAA College of Engineering and Technology, Sivakasi, Tamil nadu, India

Abstract. This research paper discusses the friction and wear behaviour of Al-12Si alloy reinforced with B_4C prepared through Powder Metallurgy (P/M) method by varying the weight percentage of reinforcement ($x = 2$, 4, 6, 8, and 10) content. The samples were prepared by using die and punch assembly and the lubricant used to eject the sample from the die was molybdenum disulfide. The compaction was done by using a compression testing machine by applying a pressure of 800 MPa. The dry sliding friction and wear behaviour of the sample was conducted on a Pin-on-Disc machine and the experimental values of friction and wear were calibrated. The Taguchi design experiment was done by applying an L25 orthogonal array for 3 factors at 5 levels for the response parameter Coefficient of Friction (CoF) and wear loss. The SEM images show the shape, size and EDX confirm the existence of Al, Si, B_4C particles in the composites. Analysis of Variance (ANOVA) for CoF of S/N ratio, shows that the reinforcement having 34.92% influence towards the S/N ratio of CoF, ANOVA for wear loss of S/N ratio shows that the sliding distance having 46.76% influence towards the S/N ratio of wear loss, when compared to that of the other two input parameters. The interaction line plot and the 2Dsurface plot for CoF and wear loss show that the increase in B_4C content decreases the wear loss and CoF. The worn surface shows that the B_4C addition will increase the wear resistance.

Key words: Al-Si, B_4C, ANOVA, Taguchi design, CoF and wear loss.

1. INTRODUCTION

Aluminium based composites are commonly utilized in manufacturing to change variations in the improvement of the tribological in addition to mechanical properties. The Al based composites are strengthened to afford extra strength to metal [1–3]. The lightweight metal Al alloy is strengthened by some of the carbide or oxide materials. Among Al alloy is the best utilized matrix metal for the planning of light weight commercial products [4–5]. Optimization of process parameters analysed by performing the milling machining of hardened steel by varying each parameter for L16 orthogonal array and output Parameter as surface finish. The result shows that radial cutting depth and the interaction between the radial and axial depth of cut are the most relevant parameters [6–7]. The face milling operation on Al6061 material according to Taguchi Orthogonal Array (OA) and Artificial Neural Network (ANN) model for various combinations of control parameter, concluded that both the experimental approaches got almost the same for surface roughness value [8–10]. The effect of cutting parameters on machine tool vibration and surface roughness was carried out in high precision CNC milling machines. Comparing the ANOVA results for full factorial and Taguchi design of experiments techniques it was found that Taguchi design of experiments is better and reliable to obtain optimal number of experiments [11–13]. Optimization of cutting process parameters increases the efficiency and improves the quality of the component [14]. The second order equation developed, and it has shown good correlation between the predicted and experimental values [15]. The Taguchi method has been successfully employed for optimizing the process parameter of milling of mild steel; it provides a systematic and efficient methodology for optimal milling parameters [16]. The CoF have been conceded out in this effort. Taguchi technique is utilized for optimization of factors and ANOVA is conceded out [17]. The friction behaviour on Al based composites utilizing Taguchi technique with load, reinforcement, sliding distance as input and output as CoF. ANOVA demonstrates the significant factors for controlling the friction.

In this research work, we discuss the Taguchi technique on dry sliding wear and friction behaviour of Al-12Si alloy reinforced with B_4C particles prepared through P/M method by varying the weight percentage of reinforcement ($x = 2$, 4, 6, 8,

*e-mail: edbertefren0420@gmail.com

Manuscript submitted 2020-03-26, revised 2020-07-08, initially accepted for publication 2020-07-30, published in December 2020

and 10) content. The Taguchi design experiment was done by applying an L25 orthogonal array for 3 factors at 5 levels for the response parameter coefficient of friction and wear loss. The ANOVA demonstrated by the S/N ratio table for CoF and wear loss was discussed and from the table it can be seen that the reinforcement plays a main role, when compared with load and sliding distance. The normal probability plot shows that the residuals fall near to the red line, which indicates that the error values were smaller in the model.

2. Experimental procedure

The Aluminium (Al) and Silicon (Si) powder was purchased from metal powder company, Thirumagalam, Madurai, Tamilnadu, India. The particle sizes of the two powders were 40 μm with purity 99.5%. The B_4C powder was purchased from sigma Aldrich, UK. The particles size of the powder was 10 μm and the powder was milled in a ball mill for 60 h to reduce the size to ≤ 100 nm. Figure 1 shows the SEM and

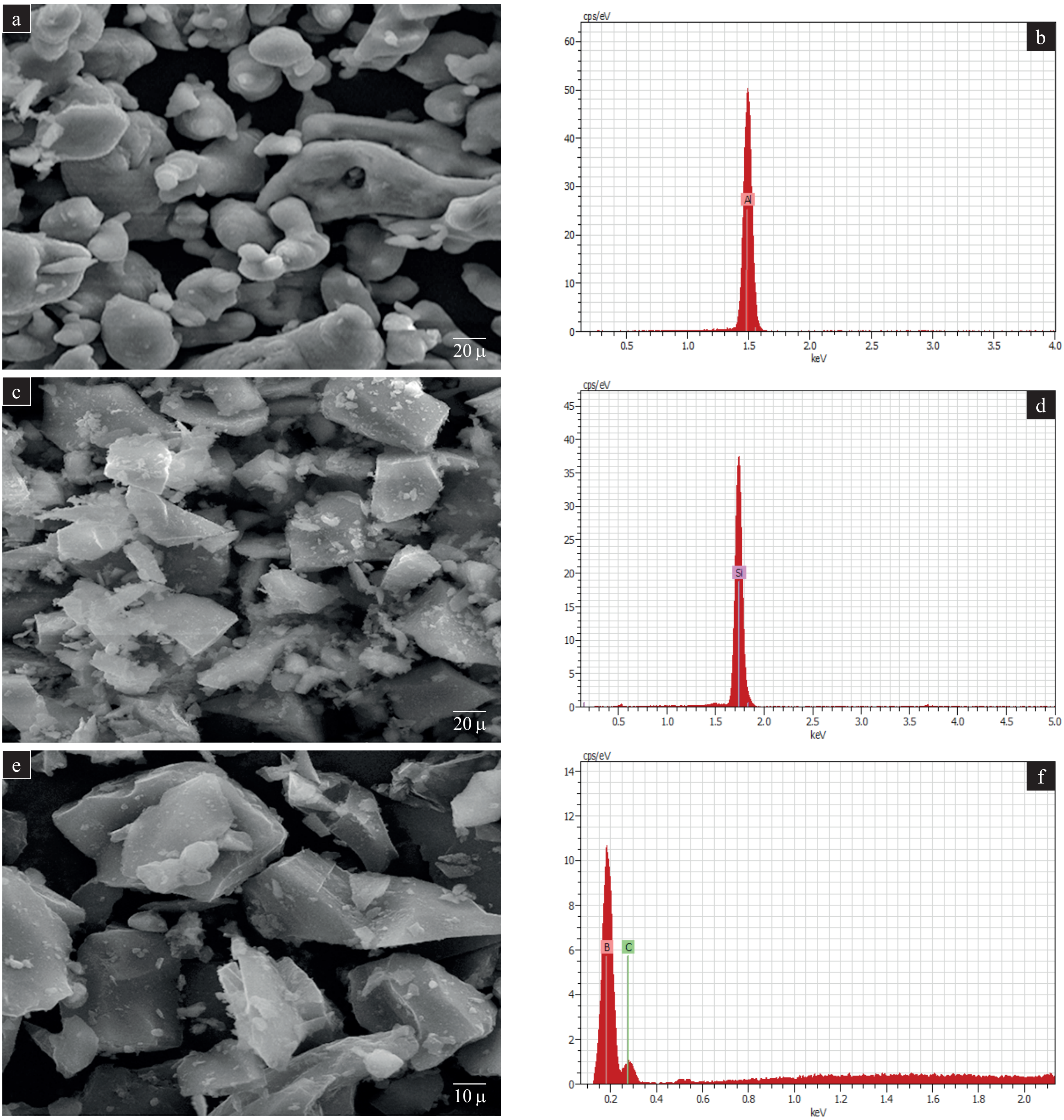

Fig. 1. Received powder SEM image (a) Al, (c) Si, and (e) B_4C, Also EDX analysis of (b) Al, (d) Si, and (f) B_4C

EDX analysis of as received powder of Al, Si, and B_4C. The powders were mixed in high energy ball mill for 30 min for homogenous mixing.

Figure 2 demonstrates the mixed powders SEM and EDX analysis of Al-Si-2B_4C, Al-Si-4B_4C, Al-Si-6B_4C, Al-Si-8B_4C, and Al-Si-10B_4C composites. The mixed powder was compacted in die and punch assembly with a pressure of 800 MPa in the compression testing machine. The samples were sintered in vacuum sintering equipment with argon gas purging with sintering temperature 500°C. The samples with 10 mm diameter and 30 mm height were used for the dry sliding friction and wear measurements on a pin-on-disc machine. During the wear test, the load was applied on the pin normal to the sliding contact of a rotating EN 31 steel disc of hardness HRC 64.

2.1. Taguchi Design. The influence of input parameters on the friction and wear loss parameters was deliberate utilizing

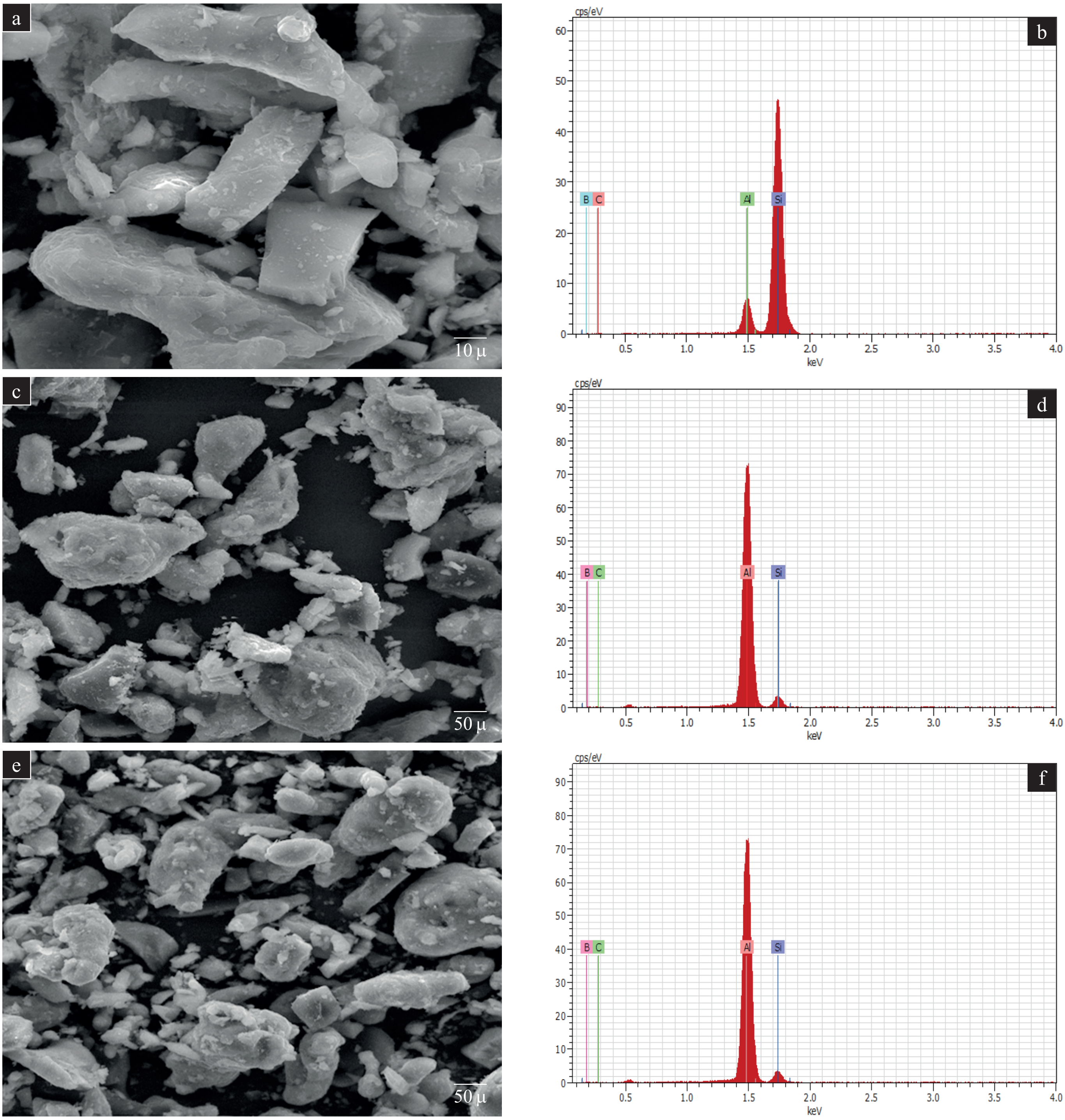

Fig. 2. Mixed powders SEM and EDX analysis of: a-b) Al-Si-2B_4C, c-d) Al-Si-4B_4C, e-f) Al-Si-6B_4C (continued on next page)

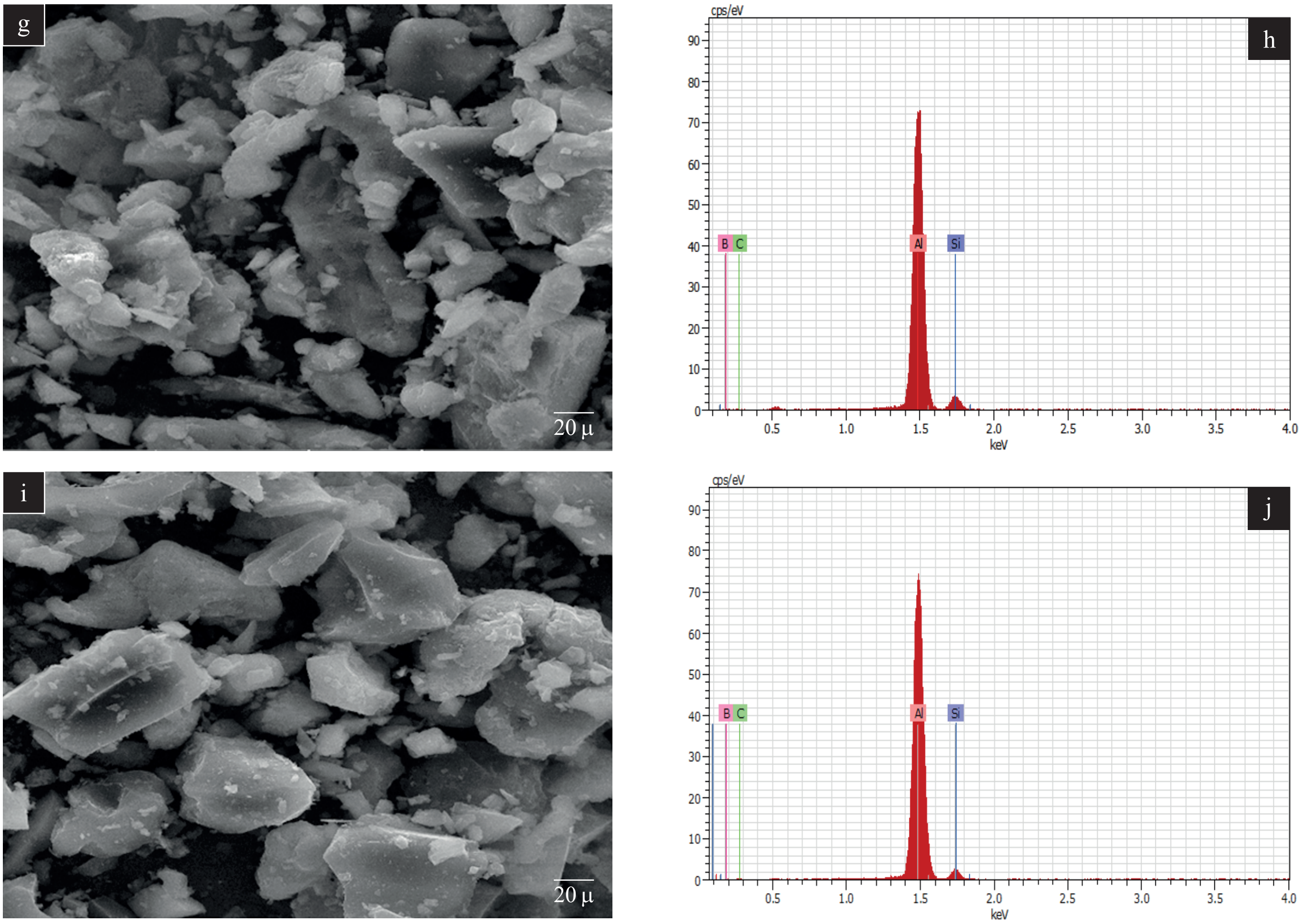

Fig. 2. Mixed powders SEM and EDX analysis of: g-h) Al-Si-8B_4C, and i-j) Al-Si-10B_4C composites

Taguchi's method. From the trial test, it was obvious to select the levels of experiments.

Table 1
Trials and levels

Factors	**Levels**				
	1	2	3	4	5
wt.% B_4C	2	4	6	8	10
Load (N)	8	16	24	32	40
SD (m)	400	800	1200	1600	2000

For the present condition, the process parameters deliberated are reinforcement, load, and SD with 3 factors at 5 levels were experimented with L25 orthogonal array. Friction and wear loss trials were shown in Table 1 for the trial plan and response for levels specified. With the design plan of L25 orthogonal array, the experimental run with reinforcement, load and sliding distance of the input parameters with the response CoF and wear loss also the S/N ratio for both responses were revealed in Table 2.

Table 2
Experimental run and response parameters

wt.% B_4C	Load (N)	SD (m)	CoF	S/N ratio	wear loss	S/N ratio
2	8	400	0.4645	6.6599	0.06531	23.6996
2	16	800	0.5148	5.7665	0.13590	17.3356
2	24	1200	0.5419	5.3209	0.25971	11.7102
2	32	1600	0.5712	4.8627	0.41114	7.7201
2	40	2000	0.6129	4.2517	0.45328	6.8725
4	8	800	0.4877	6.2369	0.08481	21.4305
4	16	1200	0.5235	5.6216	0.13732	17.2451
4	24	1600	0.553	5.1455	0.25875	11.7424
4	32	2000	0.5833	4.6816	0.33333	9.5424
4	40	400	0.5495	5.1999	0.15710	16.0761
6	8	1200	0.4903	6.1901	0.11371	18.8840
6	16	1600	0.5402	5.3488	0.20865	13.6113
6	24	2000	0.5762	4.7882	0.30424	10.3355
6	32	400	0.5256	5.5859	0.13405	17.4542

Table 2
Experimental run and response parameters

wt.% B_4C	Load (N)	SD (m)	CoF	S/N ratio	wear loss	S/N ratio
6	40	800	0.5672	4.9250	0.20609	13.7187
8	8	1600	0.4977	6.0606	0.12068	18.3671
8	16	2000	0.5340	5.4485	0.15995	15.9202
8	24	400	0.474	6.4844	0.08323	21.5935
8	32	800	0.5135	5.7891	0.15374	16.2638
8	40	1200	0.5495	5.1999	0.22239	13.0577
10	8	2000	0.4844	6.2956	0.11404	18.8585
10	16	400	0.4171	7.5947	0.05400	25.3515
10	24	800	0.4588	6.7669	0.10679	19.4289
10	32	1200	0.4866	6.2558	0.19062	14.3966
10	40	1600	0.5238	5.6162	0.24355	12.2681

3. Result and discussions

3.1. ANOVA for Coefficient of Friction of S/N ratio. The ANOVA for coefficient of friction of S/N ratio that was discussed in Table 3, the most influencing factor that influences the CoF were reinforcement B_4C compared to load and SD with the confidence level 95% for the S/N ratio of ANOVA table. The F-test value (0.05, 24, 4) = 2.7763 which is less than the F-table value 60.04; therefore, all the input factors are significant. It can also be confirmed with the percent contribution for the input factors that influence the response parameter of S/N ratio of CoF, shows that the reinforcement having 34.92% influence towards the S/N ratio of CoF, when compared to that of the other two input parameter load with 32.74% and sliding distance of 30.59%.

Table 3
Analysis of Variance for SN ratios of CoF

Source	DF	Seq SS	Adj SS	Adj MS	F-Value	P-Value	% Contribution
Wt.% B_4C	4	4.8976	4.8976	1.22439	60.04	0.0	34.92
Load (N)	4	4.5922	4.5922	1.14804	56.29	0.0	32.74
SD (m)	4	4.2903	4.2903	1.07257	52.59	0.0	30.59
Residual Error	12	0.2447	0.2447	0.02039	–	–	1.75
Total	24	14.0247	–	–	–	–	100

3.2. ANOVA for wear loss of S/N ratio. The ANOVA for wear loss of S/N ratio, that was discussed in Table 4, the most influencing factor that influences the wear loss were reinforcement B_4C compared to load and SD with the confidence level 95% for the means of ANOVA table. The F-test value (0.05, 24, 4) = 2.7763 which is less than the F-table value = 253.49, therefore, all the input factors are significant. It can also be confirmed with the percent contribution for the input factors that influence the response parameter of S/N ratio of wear loss, shows that the sliding distance having 46.76% influence towards the S/N ratio of wear loss, when compared to that of the other two input parameter load with 40.34% and reinforcement of 12.34%.

Table 4
Analysis of variance for SN ratios of wear loss

Source	DF	Seq SS	Adj SS	Adj MS	F	P	% Contri –bution
Wt.% B_4C	4	67.02	67.02	16.75	66.89	0.0	12.34
Load (N)	4	219.11	219.11	54.78	218.69	0.0	40.34
SD (m)	4	253.98	253.98	63.49	253.49	0.0	46.76
Residual Error	12	3.01	3.01	0.25	–	–	0.56
Total	24	543.12	–	–	–	–	100

3.3. Interaction Plot for Wear loss. Figure 3 shows the interaction graph of the wt.% against sliding distance the wear loss decreases due to the increase in reinforcement content B_4C, which is due to the carbon rich layer present in between the sample Al-Si-B_4C composites and the steel disc. Similarly, the interaction graph shows that the wt.% against load the wear loss decreases due to the increase in reinforcement content B_4C, and slightly increases by increase in load, this is reduced due to the carbon rich layer present in between the Al-Si-B_4C composites and the steel disc. The wear loss can be reduced and protected from hard asperities of the specimen by increasing the wt.% of B_4C from high load and sliding distance. The interaction graph shows the load against sliding distance, the wear loss increases slightly from low load to low sliding distance, but wear loss gradually increases by increasing the load and sliding distance to the maximum discussed. The carbon rich layer present in between the Al-Si-B_4C composites and the steel disc protects the sample from hard asperities and wear loss for low load and sliding distance, but for high load and sliding distance the wear loss will be more due to the hard asperities present in the surface. Similarly, the interaction graph shows that the load against wt.% the wear loss decreases due to the increase in reinforcement content B_4C, and slightly increases by increase in load, this is reduced due to the carbon rich layer present in between the Al-Si-B_4C composites and the steel disc. The wear loss can be reduced and protected from hard asperities of the specimen by increasing the wt.% of B_4C from high load and sliding distance.

The interaction graph shows that the sliding distance against load the wear loss increases slightly from low sliding distance to low load, but wear loss gradually increases by increasing the sliding distance and load to the maximum discussed. The carbon rich layer present in between the Al-Si-B_4C composites and the steel disc protects the sample from hard asperities and wear loss for low sliding distance and load, but for high sliding distance and load the wear loss will be higher due to the hard asperities present in the surface. Similarly, the interaction graph shows

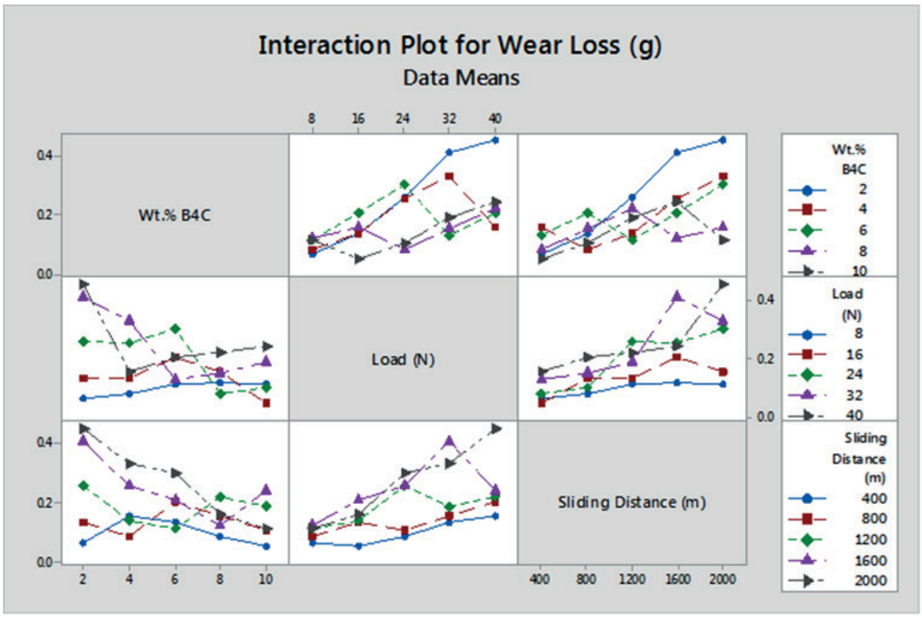

Fig. 3 The interaction plot for wear loss vs wt.%B_4C, load, sliding distance

that the sliding distance against wt.% the wear loss decreases due to the increase in reinforcement content B_4C, and slightly increases by increase in sliding distance, this is reduced due to the carbon rich layer present in between the Al-Si-B_4C composites and the steel disc. The wear loss can be reduced and protected from hard asperities of the specimen by increasing the wt.% of B_4C from high sliding distance.

3.5. Interaction Plot for coefficient of friction. Figure 4 shows the interaction graph of the wt.% against sliding distance the CoF decreases due to the increase in reinforcement content B_4C, this is due to the carbon rich layer present in between the sample Al-Si-B_4C composites and the steel disc. Similarly, the interaction graph shows that the wt.% against load the CoF decreases due to the increase in reinforcement content B_4C, and slightly increases by increase in load, this is reduced due to the carbon rich layer present in between the Al-Si-B_4C composites and the steel disc. The CoF can be reduced and protected from hard asperities of the specimen by increasing the wt.% of B_4C from high load and sliding distance.

The interaction graph shows that the load against sliding distance the CoF increases slightly from low load to low sliding

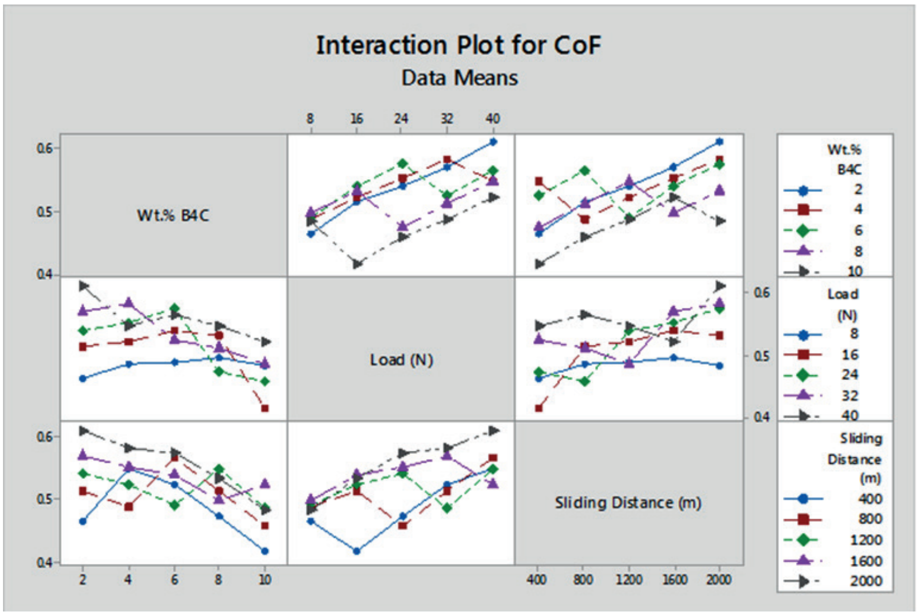

Fig. 4 The interaction plot for CoF vs wt.%B_4C, load, sliding distance

distance, but CoF gradually increases by increasing the load and sliding distance to the maximum discussed. The carbon rich layer present in between the Al-Si-B_4C composites and the steel disc protects the sample from hard asperities and CoF for low load and sliding distance, but for high load and sliding distance the CoF will be more due to the hard asperities present in the surface. Similarly, the interaction graph shows that the load against wt.% the CoF decreases due to the increase in reinforcement content B_4C, and slightly increases by increase in load, this is reduced due to the carbon rich layer present in between the Al-Si-B_4C composites and the steel disc. The CoF can be reduced and protected from hard asperities of the specimen by increasing the wt.% of B_4C from high load and sliding distance.

The interaction graph shows that the sliding distance against load the CoF increases slightly from low sliding distance to low load, but CoF gradually increases by increasing the sliding distance and load to the maximum discussed. The carbon rich layer present in between the Al-Si-B_4C composites and the steel disc protects the sample from hard asperities and CoF for low sliding distance and load, but for high sliding distance and load the CoF will be more due to the hard asperities present in the surface. Similarly, the interaction graph shows that the sliding distance against wt.% the CoF decreases due to the increase in reinforcement content B_4C, and slightly increases by increase in sliding distance, this is reduced due to the carbon rich layer present in between the Al-Si-B_4C composites and the steel disc. The CoF can be reduced and protected from hard asperities of the specimen by increasing the wt.% of B_4C from high sliding distance.

3.5. Interaction effect of 2D surface plot on CoF. Figure 5a shows the 2D surface plot of the CoF map for reinforcement vs load. The perceived CoF region was low and medium, the violet distribution was dominant. While increasing the B_4C wt% at loads, the CoF is less for the 400 m SD and marginally rises in CoF for all SD. Figure 5b demonstrates the map for reinforcement vs SD, the brown and violet distributions are identified [3]. In lower sliding distance and higher reinforcement, the brown region was identified, which confirms that increasing

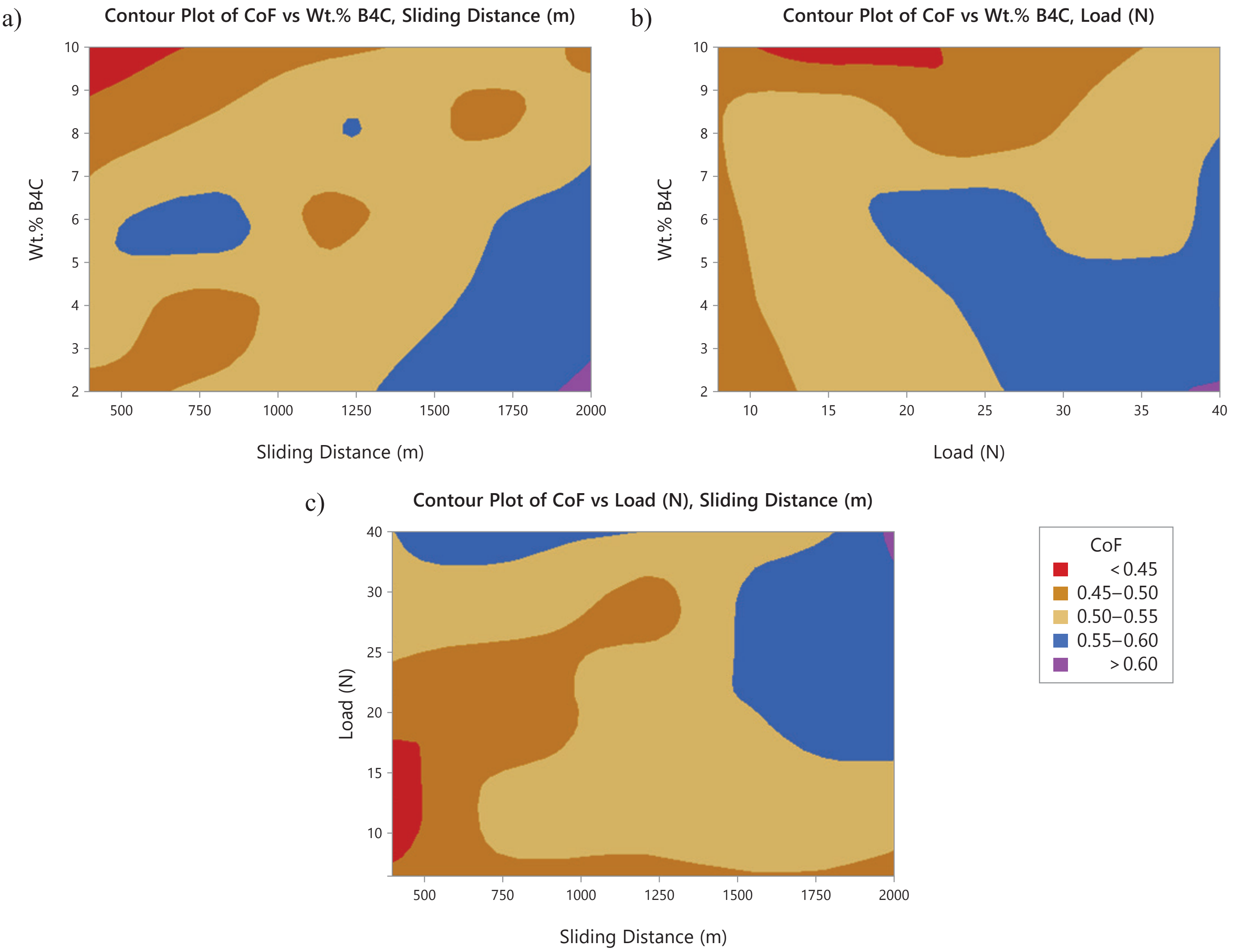

Fig. 5. 2D surface plot of B_4C wt% and the loads of 8, 16, 24, 32 and 40 N on CoF

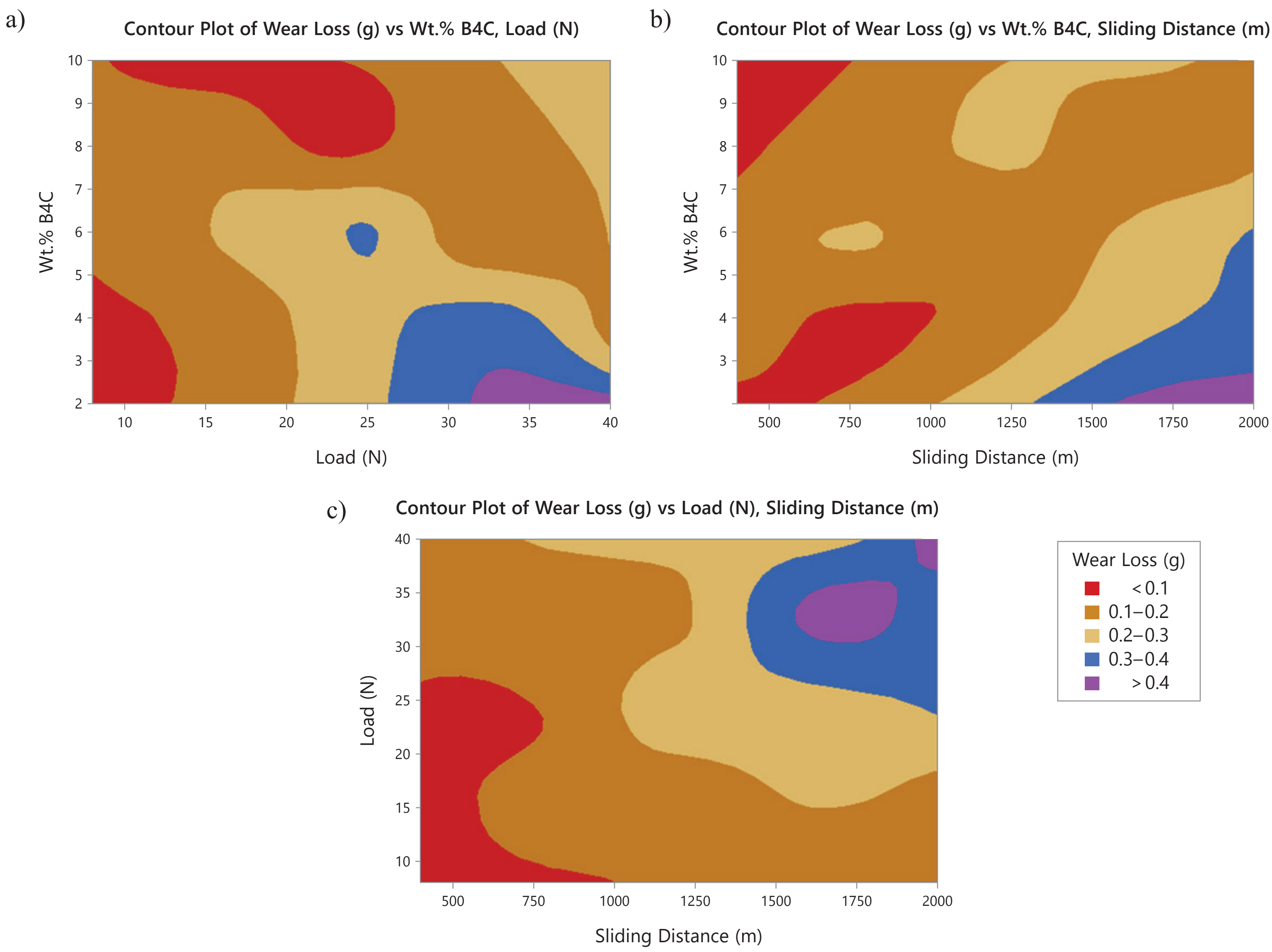

Fig. 6. 2D surface plot of B_4C wt% and the loads of 8, 16, 24, 32 and 40 N on wear loss

the SD, CoF also improved. Figure 5c shows the joined influence of load and SD on CoF for map at all reinforcements, the violet and brown region performed. Higher CoF for lower wt% of B_4C at different loads is owing to the rise in SD. This another time authorizes that the B_4C is the main supervisory factor on the CoF of the composites [12]. For the entire Al-Si-B_4C composite samples the CoF improved with the rise in the SD and load.

3.6. Interaction effect of 2D surface plot on wear loss. Figure 6 demonstrates the collaborating influence of B_4C wt% and the loads of 8, 16, 24, 32 and 40 N on wear loss. Figure 6a is the wear loss map for reinforcement vs load. The perceived wear loss region was low and medium, the violet distribution was dominant. While increasing the B_4C wt% at loads, the wear loss is less for the 400 m SD and marginally rises in wear loss for all SD. Figure 6b demonstrates the map for reinforcement vs SD, the brown and violet distributions are identified. In lower sliding distance and higher reinforcement, the brown region was identified, which confirms that increasing the SD, wear loss also improved. Figure 6c shows the joined influence of load and SD on wear loss for map at all reinforcements, the violet and brown region performed. Higher wear loss for lower wt% of B_4C at different loads owes to the rise in SD. This other time authorizes that the B_4C is the main supervisory factor on the wear loss of the composites [7]. For the entire Al-Si- B_4C composite samples, the wear loss improved with the rise in the SD and load.

3.7. Worn Surface. Figure 7 shows the optical micrograph of the worn surface of Al-Si-B_4C composites. The addition of B_4C content into the Al-Si matrix shows that the wear rate is reduced due to the carbon-rich layer and oxide debris formed at the bottom of the pin protects the pin surface and reduces the wear. Figure 7a shows delamination surface in the sliding track with heavy wear due to smaller B_4C content, if the B_4C content is increased we can see the reduction in wear and the surface of the pin becomes smoother due the carbon layer formed at the bottom of the pin and the counterpart of Figs. 7b–7e shown.

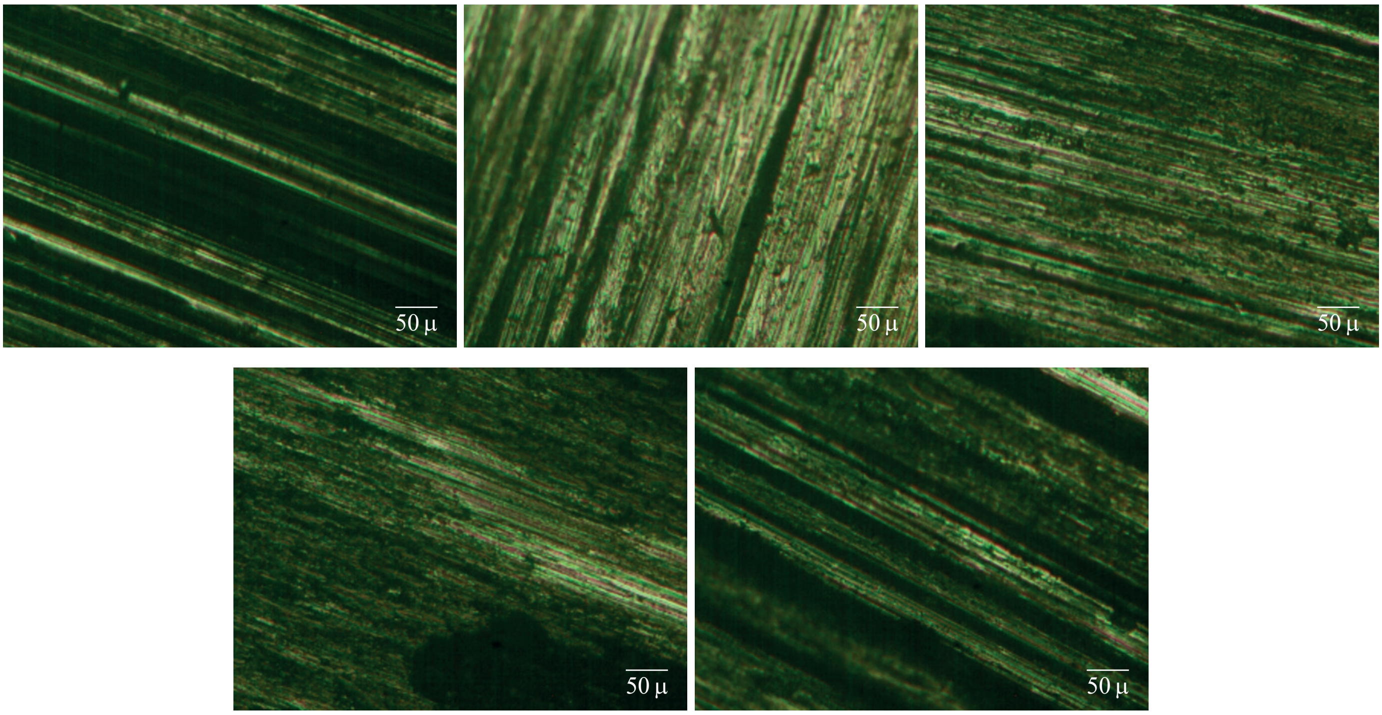

Fig. 7. Optical micrograph of worn surfaces: a) Al-12Si-2B_4C, b) Al-12Si- 4B_4C, c) Al-12Si-6B_4C, d) Al-12Si-8B_4C, e) Al-12Si-10B_4C

4. Conclusion

This current research work was focused on the dry sliding wear and friction of Al-Si-B_4C composites under powder metallurgy method using Taguchi design.

- The SEM images show the shape and size of Al, Si, B_4C particles in the composites.
- The EDX confirms the existence of the Al, Si, B_4C particles in the composites.
- ANOVA for coefficient of friction of S/N ratio, shows the reinforcement having 34.92% influence towards the S/N ratio of CoF, when compared to that of the other two input parameter loads with 32.74% and sliding distance of 30.59%.
- ANOVA for wear loss of S/N ratio, shows that the sliding distance has 46.76% influence towards the S/N ratio of wear loss, when compared to that of the other two input parameter loads with 40.34% and reinforcement of 12.34%.
- The interaction line plot and the 2D surface plot for CoF and wear loss shows that the increase in B_4C content decreases the wear loss and CoF.
- The worn surface shows that the B_4C addition will increase the wear resistance, this happens due to the carbon rich layer and oxide debris on the surface of the composite pin.

Reference

[1] C.F. John *et al*., "Corrosion behavior of ZrC particles reinforcement with Al-12Si metal matrix composites by weight loss method using acidic mediums", *Bull. Pol. Ac.: Tech*. 66(1), 9–16 (2018).

[2] J.E. Ribeiro, M.B. Cesar, and H. Lopes, "Optimisation of machining parameters to improve the surface quality", *Procedia Struct. Integrity* 5, 355–362 (2017).

[3] M. Chmielewski, K. Pietrzak, A. Strojny-Nędza, D. Jarząbek, and S. Nosewicz, "Investigations of interface properties in copper-silicon carbide composites", *Arch. Metall. Mater*. 62(2B), 1315–1318 (2017).

[4] M.S. Sukumar, P.V. Ramaiah, and A. Nagarjun, "Optimization and prediction of parameters in face milling of Al-6061 using Taguchi and ANN approach", *Procedia Eng.* 97, 365–371 (2014).

[5] T. Mugilan, M.S. Aezhisai Vallavi, S. Santhosh, D. Sugumar, and S. Christopher Ezhil Singh, "Machining of microholes in Ti-6Al-4V by hybrid micro-EDM to improve process parameters and flushing properties", *Bull. Pol. Ac.: Tech*. 68(3), 565–573 (2020).

[6] M. Subramanian, M. Sakthivel, K. Sooryaprakash, and R. Sudhakaran, "Optimization of end mill tool geometry parameter for Al7075-T6 machining operation based on vibration amplitude by response surface methodology", *Measurement* 46(10), 4005–4022 (2013).

[7] M. Chmielewski *et al*., "Effect of metallic coating on the properties of copper-silicon carbide composites", *Appl. Surf. Sci.* 421(A1), 159–169 (2017).

[8] R. Lmalghan, K. Rao M C, A. Kumar S., Shrikantha S. Rao, and M.A. Herbert, "Machining parameters optimization of AA6061 using response surface methodology and particle swarm optimization", *Int. J. Precis. Eng. Manuf.* 19(5), 695–704 (2018).

[9] K. Prasadraju, M. Satish Raja, V. Praveen, and I. Ajith Kumar, "Optimization of process parameter for milling operation using Taguchi method", *Int. J. of Eng. Trends and Technol*. 48(1), 1–6 (2017)

[10] S. Christopher Ezhil Singh and N. Selvakumar, "Optimization and effect of dry sliding wear and friction behavior, electrical resistivity and mechanical properties of Cu–4Cr–xZrC composites", *J. Appl. Res. Technol*. 16(4), 299–311 (2019).

[11] M.A. Subraj, J.B. Raj, S. Christopher Ezhil Singh, "Friction behavior of Al-Si-B_4C composites prepared by powder metallurgy technique using RSM", *Int. J. of Mech. Eng. and Technol*. 9(11), 1339–1349 (2018).

[12] M. Chmielewski *et al*.,"Analysis of the micromechanical properties of copper-silicon carbide composites using nano- indentation measurements", *Ceram. Int*. 45(7), 9164–9173 (2019).

[13] M.A. Subraj, J.B. Raj, S. Christopher Ezhil Singh, "Effect of wear behavior on B_4C particles reinforced with Al-Si alloy prepared through powder metallurgy method using response surface methodology", *Int. J. of Mech. and Prod. Eng. Res. Develop.* 9(1), 41–50 (2018).

[14] S. Christopher Ezhil Singh and N. Selvakumar, "Effect of milled B_4C nanoparticles on tribological analysis, microstructure and mechanical properties of Cu–4Cr matrix produced by hot extrusion", *Arch. Civ. Mech. Eng.* 17(2), 446–456 (2017).

[15] N. Selvakumar and S. Christopher Ezhil Singh, "Influence of nano ZrC content on tribological analysis, microstructure and mechanical properties of Cu–4Cr matrix composites produced by hot extrusion", *Arch. Civ. Mech. Eng.* 16(3), 537–552 (2016).

[16] C. Sankar, K. Gangatharan, and S. Christopher Ezhil Singh, "Optimization on tribological behavior of milled nano B_4C Particles reinforced with AZ91 alloy through powder metallurgy method", *Trans. Indian Inst. Met*. 72(5), 1255–1275 (2019).

[17] C.F. John, R.C. Paul and S. Christopher Ezhil Singh, "Tribological behavior, mechanical properties and microstructure of Al-12Si-ZrC composite prepared by powder metallurgy", *Bull. Pol. Ac.: Tech*. 65(2), 149–154 (2017).